

Electron momentum density in $\text{Ni}_{75}\text{Cu}_{25}$ and $\text{Ni}_{75}\text{Co}_{25}$ disordered alloys: a high-resolution Compton-scattering study

This article has been downloaded from IOPscience. Please scroll down to see the full text article.

2005 J. Phys.: Condens. Matter 17 6425

(<http://iopscience.iop.org/0953-8984/17/41/013>)

View [the table of contents for this issue](#), or go to the [journal homepage](#) for more

Download details:

IP Address: 129.252.86.83

The article was downloaded on 28/05/2010 at 06:10

Please note that [terms and conditions apply](#).

Electron momentum density in $\text{Ni}_{75}\text{Cu}_{25}$ and $\text{Ni}_{75}\text{Co}_{25}$ disordered alloys: a high-resolution Compton-scattering study

J Kwiatkowska¹, L Dobrzyński^{2,3}, A Andrejczuk², E Żukowski²,
Ch Bellin⁴, G Loupiaz⁴, A Shukla^{5,6} and Th Buslaps⁵

¹ Henryk Niewodniczański Institute of Nuclear Physics, Polish Academy of Sciences, Radzikowskiego 152, 31-342 Kraków, Poland

² Institute of Experimental Physics, University of Białystok, Lipowa 41, 15-424 Białystok, Poland

³ The Soltan Institute for Nuclear Studies, 05-400 Otwock-Świerk, Poland

⁴ Laboratoire de Mineralogie et Cristallographie, University Paris 6, Place Jussieu 4, Paris, France

⁵ European Synchrotron Radiation Facility, BP220, 38043 Grenoble, France

Received 20 July 2005, in final form 9 September 2005

Published 30 September 2005

Online at stacks.iop.org/JPhysCM/17/6425

Abstract

We report high-resolution Compton profiles (CPs) of $\text{Ni}_{75}\text{Cu}_{25}$ and $\text{Ni}_{75}\text{Co}_{25}$ disordered, ferromagnetic alloys measured along [100], [110] and [111] crystallographic directions. The directional CP anisotropies, profile derivatives and reciprocal form factors $B(z)$ are analysed in detail and compared with first-principles KKR-CPA (Korringa–Kohn–Rostoker coherent potential approximation) calculations. Good overall agreement is found between the experimental and theoretical anisotropies. It follows from experiment that the majority-spin Fermi surface of the $\text{Ni}_{75}\text{Cu}_{25}$ and $\text{Ni}_{75}\text{Co}_{25}$ alloys occurs at higher momentum than the theory predicts. Also, a splitting in the secondary maxima in experimental $B(z)$ functions of the alloys is observed, which is not predicted by the KKR-CPA calculations.

1. Introduction

Compton scattering is widely used to determine the ground-state electronic properties of solids [1]. As the method is not sensitive to defects or impaired by high impurity concentration it can be successfully applied to study disordered, nondilute alloys [2–9]. On the other hand, the high resolution (of the order of 0.1 au, atomic units of momentum) currently attainable in synchrotron-based Compton scattering experiments coupled with high statistical accuracy makes the method a sensitive tool to probe subtle fermiological properties of materials.

The quantity measured in a Compton scattering experiment is the so called Compton profile, $J(p_z)$, which under conditions of the impulse approximation [10, 11] gives direct

⁶ Present address: Laboratoire de Mineralogie et Cristallographie, University Paris 6, Place Jussieu 4, Paris, France.

access to the momentum distribution of the scattering system. In this approximation the $J(p_z)$ is an integral of the momentum density $\rho(\mathbf{p})$ over $p_x p_y$ planes perpendicular to the direction p_z defined by the experimental scattering vector, i.e.

$$J(p_z) = \int \int \rho(\mathbf{p}) \, dp_x \, dp_y,$$

where

$$\rho(\mathbf{p}) = (2\pi)^{-3} \sum_i \left| \int \psi_i(\mathbf{r}) \exp(i\mathbf{p} \cdot \mathbf{r}) \, d^3r \right|^2$$

and $\psi_i(\mathbf{r})$ denotes the ground-state electron wavefunction. The summation extends over all occupied states. When the experiment is done on a single-crystal sample, p_z is aligned with a crystallographic direction of interest.

How specific Fermi surface (FS) features are reflected in the Compton profiles has been demonstrated by many authors; see for example [12–14]. Generally speaking FS effects can produce sharp structure in the profile and this structure may be repeated in a periodic system whenever the $p_x p_y$ plane crosses the same portions in secondary FSs encountered in Brillouin zones centred on neighbouring reciprocal lattice points.

As mentioned above, the Compton scattering measurements have been performed on disordered alloys before; however, not much is known about similar studies in the case of alloys exhibiting magnetic order. In the present article we discuss Compton profiles of two magnetic, disordered alloys $\text{Ni}_{75}\text{Cu}_{25}$ and $\text{Ni}_{75}\text{Co}_{25}$, measured with high momentum resolution (0.15 au) at the synchrotron radiation source (European Synchrotron Radiation Facility, ESRF). The systems were previously investigated [2] theoretically by the KKR-CPA method (see [15–17] and references therein) and experimentally with the use of a low resolution (0.4 au) gamma-ray Compton spectrometer. The computations were parameter free, with a high level of charge and spin self-consistency, and included effects of magnetic ordering. Spin-resolved Compton profiles were obtained and the results lead to the conclusion that the majority-spin contribution to the profiles of both alloys is nearly the same and that changes in the profiles upon alloying Ni with either Cu or Co is due to minority-spin contributions. It was also found that the alloying mostly influences d states, with the s and p states undergoing only little change. The 0.4 au resolution proved insufficient to reveal fine structure in the directional anisotropies predicted by the theory. It was postulated that high-resolution measurements were necessary to interpret fine details in the calculated profiles and to verify the theoretical findings.

2. Experimental details

High-resolution Compton profiles along three main crystallographic directions for each of the two, $\text{Ni}_{75}\text{Cu}_{25}$ and $\text{Ni}_{75}\text{Co}_{25}$ alloys were measured at the ESRF, in Grenoble, on a high-energy beamline (ID15B), using the Compton scanning spectrometer [18]. The samples were single crystals prepared in the way described in [2]. The energy of incident photons was set to 55.8 keV by the use of a Si(311), horizontally focusing, Bragg-type bent monochromator crystal. The scattering angle was 175° . The collected Compton spectra were energy analysed using the Ge(440) analyser crystal and detected by a NaI scintillator counter. The number of counts collected at the maximum of the Compton profile, at 46.77 keV, was about 5×10^5 . The energy-dependent resolution of 0.15 au at the Compton peak was deduced from the full width at half maximum of the elastic line, which in this case was $\text{FWHM} = 0.22$ au.

After subtracting the background, the raw data were corrected for all energy-dependent terms, such as absorption in analyser and detector, detector efficiency and analyser

reflectivity [19]. The energy scale was next converted into a momentum scale. After normalization to the number of electrons per formula unit, the contribution due to multiple scattering, i.e. photons that are Compton-scattered more than once, was subtracted from the measured total profile. Both elastic and inelastic contributions to the multiple-scattering were calculated using a Monte Carlo simulation which took into account beam polarization, sample geometry and sample density [20].

In order to obtain the valence-electron Compton profiles, the calculated atomic-core Compton profile was subtracted from the total corrected measured profile.

3. Results and discussion

In the discussion of our results we refer to the theoretical findings of paper [2] obtained using the KKR-CPA formalism. In particular, fine details in the calculated anisotropy of Ni₇₅Cu₂₅ and Ni₇₅Co₂₅ (shown in figures 6–8 of [2]) will be compared with experimental, high-resolution Compton profile anisotropies of the present study. These were determined in the usual way by taking differences between the valence-electron profiles for the three main crystallographic directions i.e. [110]–[100], [111]–[110] and [111]–[100], and are presented in figures 1 and 2. For comparison, the calculated total anisotropies are also plotted, left unbroadened by experimental resolution, to clearly show where fine structure is to be expected.

Theoretical anisotropies from spin-resolved calculations are presented in [2] as split into majority (up-spin) and minority (down-spin) state contributions to reveal the role of magnetism in the profile evolution when Ni is alloyed with nonmagnetic (Cu) and magnetic (Co) atoms. The anisotropies involving the [110] direction are the highest and thus the most interesting; any d-bonding present in the samples will be along this direction and will contribute to the anisotropy. The interesting regions are 1–2 and 2–4 au. The contributions from up-spin states are smooth and similar in Ni and the alloys (see figures 6–8 of [2]), and it is mainly down-spin contributions that have a bearing on the shape of the total anisotropy. Thus any differences in anisotropy between the alloys are mainly due to the differences in their down-spin anisotropy. As can be seen, the high-resolution experimental anisotropies shown in figures 1 and 2 exhibit the same features as the theoretical anisotropies. The first main oscillation in Ni₇₅Cu₂₅ is smooth and without any structure, while the one in Ni₇₅Co₂₅ shows a hump, an imprint of the structure in the down-spin contribution. A similar shoulder is also present in the second oscillation, between 2.4 and 3.2 au, likewise in agreement with the theoretical calculations. The fine structure in anisotropy predicted by the theory is reproduced by the high-resolution experiment, thus supporting the theoretical findings.

The high-resolution results show other interesting features in the anisotropies which are also in accordance with the theory. As indicated by Wang and Callaway [12], much of the fine structure in anisotropies can be attributed to specific portions of the Fermi surface. Thus the structure present near 0.27 and 0.82 au in [111]–[110] anisotropy (originating from structure in $J(111)$) calculated for pure Ni [12] can be associated with the L_2' necks of the Ni Fermi surface. The same fine features (pointed out by arrows in figures 1(b), (c) and 2(b), (c)) are present in our measured as well as calculated anisotropies of both alloys, pointing to the good level of agreement between the experiment and theory and to the sensitivity of the measurement with 0.15 au resolution to the topology of the Fermi surface. An excellent agreement between the experiment and the theory in anisotropies of Ni₇₅Co₂₅ at low momenta (below 1 au), the region essentially related to the features of the primary Fermi surface, is noteworthy.

In order to see Fermi breaks we follow the idea described in [13] and present the derivatives of Compton profiles with respect to momentum along all the measured directions; see figures 3 and 4.

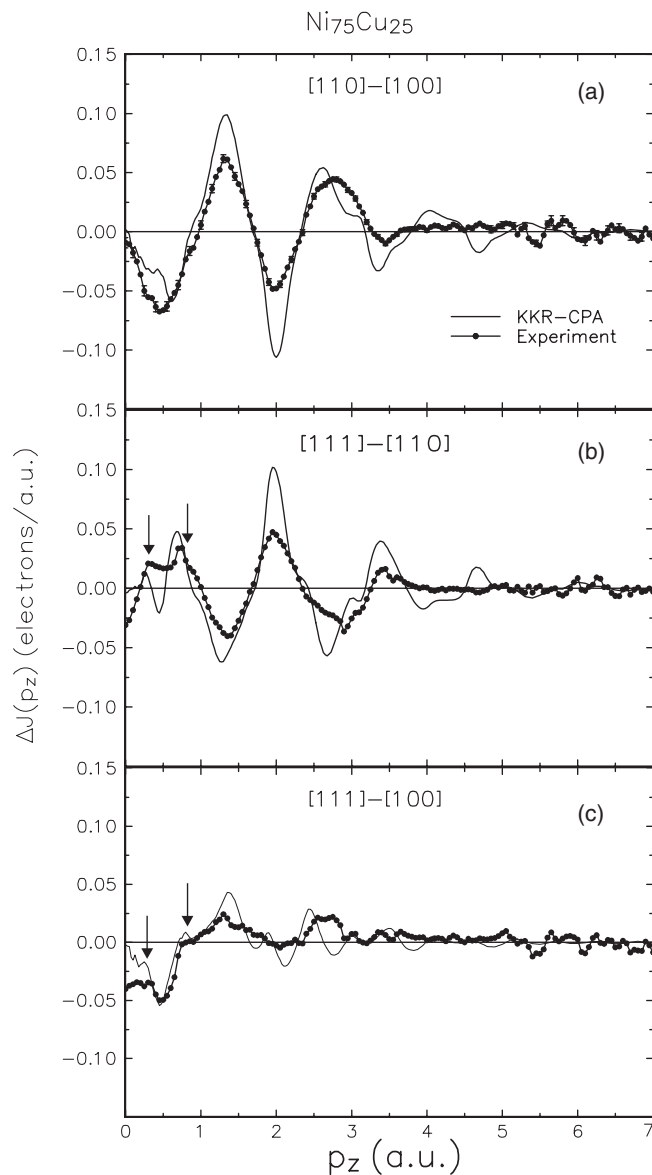


Figure 1. Directional anisotropies of Compton profiles of $\text{Ni}_{75}\text{Cu}_{25}$ alloy; experimental data are compared with theoretical results. The theoretical curves are not convoluted with the experimental resolution function to emphasize details in the fine structure. The arrows indicate where the structure associated with $L_{2'}$ necks can be expected.

The derivatives of the theoretical profiles are also included. It is striking to see that in all cases the first minimum, related to the crossing of the (sp)-sheet of the Fermi surface, appears at larger momentum than predicted by theory (solid lines). This may indicate swelling of the Fermi surface of the alloys by about 10–15% with respect to that theoretically predicted. We also note that the experimental and theoretical derivatives calculated much beyond this Fermi momentum agree quite well with each other. This is especially true for the major oscillatory structure of dJ/dp_z . The differences seen in minor oscillations are quite pronounced; however,

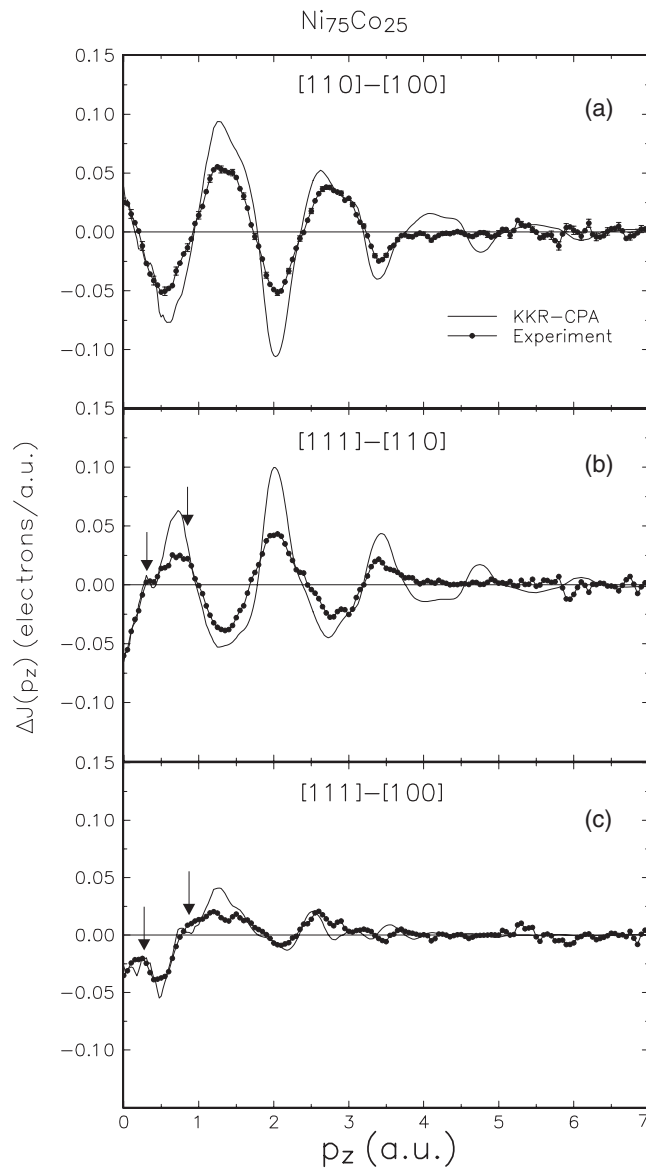


Figure 2. The same as figure 1 for Ni₇₅Co₂₅ alloy.

these are difficult to interpret because of the complexity of the shape of the Fermi surface of the studied alloys. It can be stated that the general trend predicted by the theory is clearly followed by the experiment.

As pointed out by Wang and Callaway [12], in the case of nickel the outer ($sp\uparrow$) sheet of the Fermi surface is flat and nearly perpendicular to the [110] direction over a large portion of the Brillouin zone (see figure 5 of [21]). Thus significant structure will be produced in $J(110)$ when the plane perpendicular to the [110] axis crosses the sheet, which is at $p_z = 0.59$ au in the case of Ni, and repetitions of this structure can be expected near 1.93 and 3.26 au associated with zones centered at (111) and (220) reciprocal lattice points, respectively. The minima

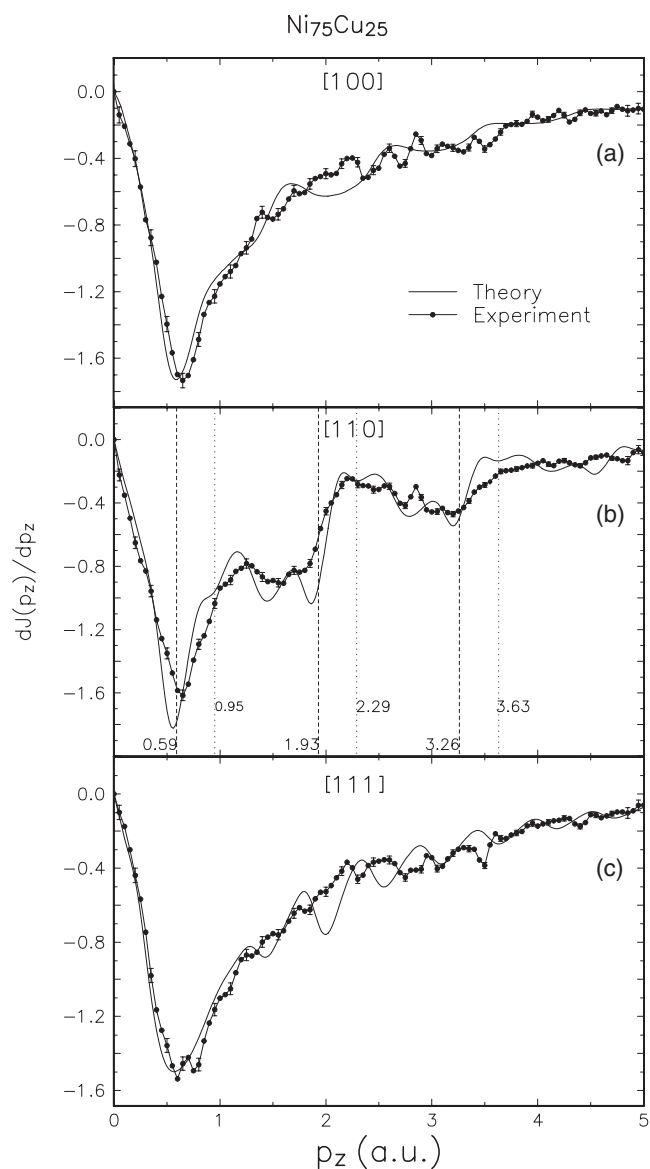


Figure 3. First derivatives dJ/dp_z of the Compton profiles of $\text{Ni}_{75}\text{Cu}_{25}$ alloy. Theoretical profiles are resolution broadened prior to taking the derivative.

observed in $[110]$ – $[100]$ anisotropy are attributed in [12] to these crossings. Similar structure, however much weaker, associated with d-sheet crossing would be expected near 0.95 au, and its repetitions around 2.29 and 3.63 au (as deduced from the FS of Ni, presented in [21]). The minima ascribed to the sp-sheet crossings are found in the anisotropy of the studied alloys at very similar p_z values as those for pure nickel. The crossings are also seen on the derivative of our experimental $[110]$ profiles in figures 3(b) and 4(b). For reference, the positions of the crossings in Ni are marked with vertical lines (dashed lines). The dotted lines mark the d-sheet crossings in nickel. It can be noted that the minima and deflections in derivatives for the alloys fall rather close to the ones for Ni. The theoretical curves show sharper features at

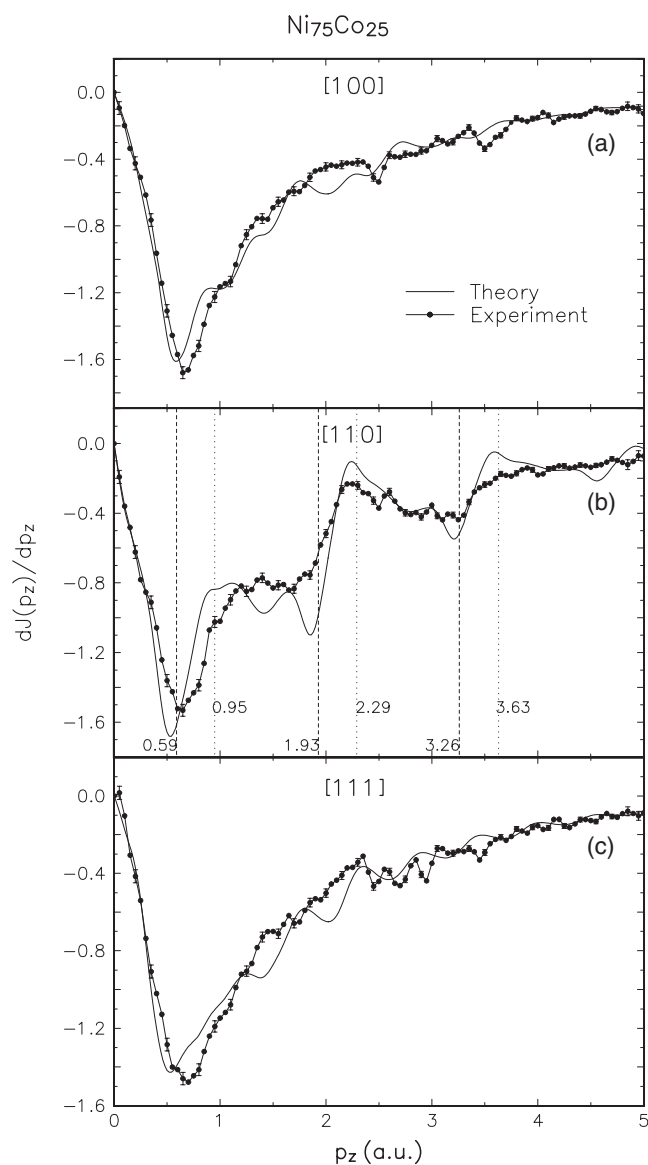


Figure 4. The same as figure 3 for Ni₇₅Co₂₅ alloy.

the crossings than those obtained from the experiment, especially for repetitions in the higher zones; however, theory is known to generally overestimate these contributions.

In order to understand better the role of d electrons we discuss Fourier transformed Compton profiles, the so called ‘*B*-functions’, defined as

$$B(z) = \int J(p_z) \exp(-ip_z z) dp_z,$$

for the [110] direction of both Ni₇₅Cu₂₅ and Ni₇₅Co₂₅ alloys.

The properties of the *B*-function introduced by Pattison *et al* [22], also called a reciprocal form factor or autocorrelation function, were widely discussed by many authors (see for example [23–26]). In a metal the behaviour of this function near the lattice vectors reflects

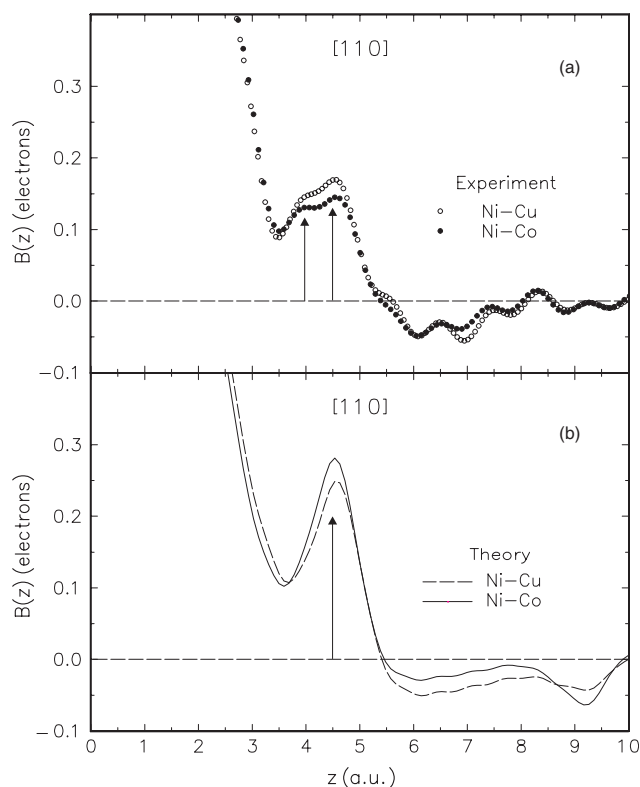


Figure 5. Experimental and calculated $B(z)$ functions along the $[110]$ direction for the $\text{Ni}_{75}\text{Cu}_{25}$ and $\text{Ni}_{75}\text{Co}_{25}$ alloys. The arrows mark the positions of experimental secondary maxima found in pure Cu and Ni (after [27]). The error bars in (a) are smaller than the size of the experimental points.

the properties of electrons in the uppermost occupied bands, i.e. the electrons determining the shape of the Fermi surface. As argued by Pattison *et al* [26], any secondary peaks centred on the lattice sites must originate from the electrons in the unfilled band. When the band is a hybrid of free electrons and d electrons, due to the more localized nature of the latter secondary maxima around translational lattice sites can be observed, superimposed on a uniform contribution from the free electrons. Pattison *et al* [26] and later Rollason *et al* [27] determined B -functions for $[110]$ Compton profiles of Cu and Ni respectively. Both results reveal a secondary maximum localized just below the first lattice translation site in the $[110]$ direction (see figure 7 in [27]). On the $B(z)$ rapidly decaying with increasing distance z , and due to sp electrons, a ‘shoulder’ is observed in the region 3.5–5 au. This shoulder exhibits a clear maximum at about 4.5 au in the case of Ni. A similar maximum, however much less pronounced, appears in $B(z)$ of Cu at lower values of z , just below 4 au.

The common feature found for Cu and Ni was that the experimental values of $B(z)$ along the $[110]$ direction were lower than the ones predicted by theory, and the differences were attributed to improper theoretical description of the electron–electron correlation effects.

Considering the above it was interesting to examine the behaviour of the $B(z)$ function in the studied alloys. The results for both $\text{Ni}_{75}\text{Cu}_{25}$ and $\text{Ni}_{75}\text{Co}_{25}$ alloys are displayed in figure 5.

It can be seen that the secondary maximum in the same z region, 3.5–5 au, is observed in each alloy, in both experiment and theory. Two features are noteworthy. The experiment

shows, figure 5(a), that the maximum in Ni₇₅Cu₂₅ is higher than in Ni₇₅Co₂₅. This is reversed in the theoretical result shown in figure 5(b). The reason for this is not clear. The second important feature is that the experimental maximum shows apparent splitting. Interestingly, the two shoulders are in positions where maxima for Cu and Ni were found in the relevant experimental $B(z)$ functions (marked with arrows). In the case of Ni₇₅Cu₂₅ it could be argued that the maxima appear as if nickel and copper made separate contributions to the B -function of the alloy. However, the fact that the shoulders in Ni₇₅Co₂₅ alloy look much the same indicates that the origin of the splitting is more subtle and probably indicates a common feature of d-bands. In the interpretation of $B(z)$ in [26] this function was approximated by a product of two functions: one reflecting the properties of the Brillouin zones (or Fermi surfaces), and the other depending on the autocorrelation function of the periodic part of the Bloch functions. One can note that the Bloch functions could be constructed, at least at the initial stage of calculations, from individual functions of the alloy elements. Thus the autocorrelation functions for the Bloch functions can exhibit more structure than the ones describing pure Ni, Co or Cu metals. Also the elements in the alloy can contribute differently to the electronic states close to the Fermi level, which can also influence the behaviour of the $B(z)$. Were this true, it would show that the Compton scattering can add important and unique information on individual properties of impurity atoms in metals. Certainly the observed effects call for independent theoretical study.

In the context of this work it is worth mentioning an interesting study of the Ni–Cu system by Metz *et al* [28], who observed directly the effects of alloying close to the Fermi energy, using the $(\gamma, e\gamma)$ coincidence technique. Their observations generally agree with the predictions of KKR-CPA theory; however, it is difficult to compare them directly with our results, mainly because of the very different composition of the alloys studied.

4. Conclusions

By performing the high-resolution Compton scattering experiments and displaying good agreement of the fine structure of the Compton profile anisotropy of Ni₇₅Cu₂₅ and Ni₇₅Co₂₅ with theory, we confirmed the theoretical findings reported in [2] that the changes upon the addition of Cu or Co impurities to Ni are limited mainly to the changes in the minority-spin states. On the other hand, the experimental results clearly show that the majority-band Fermi surface of the alloys has bigger dimensions than theory predicts, as indicated by the position of FS crossings represented by the minima in the profile derivatives. In addition, the splitting in the secondary maxima of unknown origin was detected in the experimental $B(z)$ functions of the alloys, which requires further theoretical analysis.

Acknowledgments

The authors are grateful to S Kaprzyk and B Bansil for the KKR-CPA calculations of the Compton profiles of Ni₇₅Cu₂₅ and Ni₇₅Co₂₅ alloys. Also we thank F Maniawski, whose contribution to the single-crystal growth and to the samples' preparation is highly appreciated.

References

- [1] Cooper M J *et al* (ed) 2004 *X-Ray Compton Scattering* (Oxford: Oxford University Press)
- [2] Bansil A, Kaprzyk S, Andrejczuk A, Dobrzyński L, Kwiatkowska J, Maniawski F and Żukowski G 1998 *Phys. Rev. B* **57** 314–23

- [3] Stutz G, Wohler F, Kaprolat A, Schülke W, Sakurai Y, Tanaka Y, Ito M, Kawata H, Shiotani N, Kaprzyk S and Bansil A 1999 *Phys. Rev. B* **60** 7099–112
- [4] Matsumoto I, Kwiatkowska J, Maniawski F, Bansil A, Kaprzyk S, Itou M, Kawata H and Shiotani N 2000 *J. Phys. Chem. Solids* **61** 375–8
- [5] Matsumoto I, Kwiatkowska J, Maniawski F, Itou M, Kawata H, Shiotani N, Kaprzyk S, Mijnen P E, Barbiellini B and Bansil A 2001 *Phys. Rev. B* **64** 045121
- [6] Matsumoto I, Kawata H and Shiotani N 2001 *Phys. Rev. B* **64** 195132
- [7] Suortti P, Buslaps T, Honkimäki V, Shukla A, Kwiatkowska J, Maniawski F, Kaprzyk S and Bansil A 2001 *J. Phys. Chem. Solids* **62** 2223–31
- [8] Samsel-Czekala M, Kontrym-Sznajd G, Döring G, Schülke W, Kwiatkowska J, Maniawski F, Kaprzyk S and Bansil A 2003 *Appl. Phys. A* **76** 87–92
- [9] Kwiatkowska J, Maniawski F, Matsumoto I, Kawata H, Shiotani N, Lityńska L, Kaprzyk S and Bansil A 2004 *Phys. Rev. B* **70** 075106
- [10] Platzman P M and Tzoar N 1965 *Phys. Rev.* **139** A410–3
- [11] Eisenberger P and Platzman P M 1970 *Phys. Rev. A* **2** 415–23
- [12] Wang C S and Callaway J 1975 *Phys. Rev. B* **11** 2417–20
- [13] Sakurai Y, Tanaka Y, Bansil A, Kaprzyk S, Stewart A T, Nagashima Y, Hyodo T, Nanao N, Kawata H and Shiotani N 1995 *Phys. Rev. Lett.* **74** 2252–55
- [14] Ohata T, Itou M, Matsumoto I, Sakurai Y, Kawata H, Shiotani N, Kaprzyk S, Mijnen P E and Bansil A 2000 *Phys. Rev. B* **62** 16528–35
- [15] Bansil A 1993 *Z. Naturf. a* **48** 165–79
- [16] Kaprzyk S and Bansil A 1990 *Phys. Rev. B* **42** 7358–62
- [17] Bansil A, Kaprzyk S and Toboła J 1992 *Mater. Res. Soc. Symp. Proc.* **253** 505
- [18] Suortti P, Buslaps T, Fajardo P, Honkimäki V, Kretschmer M, Lienert U, McCarthy J E, Renier M, Shukla A, Tschentscher Th and Meinander T 1999 *J. Synchrotron Radiat.* **6** 69–80
- [19] Balibar F, Epelboin Y and Malgrange C 1975 *Acta Crystallogr. A* **31** 836
- [20] Chomilier J, Loupiau G and Felsteiner J 1985 *Nucl. Instrum. Methods A* **235** 603
- [21] Wang C S and Callaway J 1974 *Phys. Rev. B* **9** 4897–907
- [22] Pattison P, Weyrich W and Williams B G 1977 *Solid State Commun.* **21** 967
- [23] Cooper M J 1985 *Rep. Prog. Phys.* **48** 415–81
- [24] Schülke W 1977 *Phys. Status Solidi b* **82** 229
- [25] Pattison P and Weyrich W 1979 *J. Phys. Chem. Solids* **40** 213
- [26] Pattison P, Hansen N K and Schneider J R 1982 *Z. Phys. B* **46** 285–94
- [27] Rollason A J, Schneider J R, Laundry D S, Holt R S and Cooper M J 1987 *J. Phys. F: Met. Phys.* **17** 1105–21
- [28] Metz C, Tschentscher Th, Sattler T, Höppner K, Schneider J R, Wittmaack K, Frischke D and Bell F 1999 *Phys. Rev. B* **60** 14049–56